

Cite this: *Mater. Adv.*, 2026,  
7, 3350

# Reaction and recovery of nucleation particle strontium chloride hexahydrate in calcium chloride hexahydrate

Denali Ibbotson  and Patrick J. Shamberger \*

Isostructural solid phases with similar lattice parameters are known to promote nucleation in salt hydrate phase change material (PCM) systems, as they serve as templates for crystal growth. However, the phases with the closest structural and chemical similarities are generally also salt hydrates and thus, are susceptible to dissolution or reaction to form phases with different hydration states. Here, we investigate an isostructural system where the candidate nucleation particle, strontium chloride hexahydrate ( $\text{SrCl}_2 \cdot 6\text{H}_2\text{O}$ ), reacts in the liquid PCM, calcium chloride hexahydrate ( $\text{CaCl}_2 \cdot 6\text{H}_2\text{O}$ ). We demonstrate that when present, crystalline  $\text{SrCl}_2 \cdot 6\text{H}_2\text{O}$  dramatically reduces undercooling of  $\text{CaCl}_2 \cdot 6\text{H}_2\text{O}$ . However, when present in low concentrations,  $\text{SrCl}_2 \cdot 6\text{H}_2\text{O}$  will react with  $\text{CaCl}_2 \cdot 6\text{H}_2\text{O}$  to form a lower hydrate phase,  $\text{SrCl}_2 \cdot 2\text{H}_2\text{O}$ , which does not promote nucleation in the system. Critically, we demonstrate that it is possible to regain the nucleation particle activity by supercooling the system, recovering the active  $\text{SrCl}_2 \cdot 6\text{H}_2\text{O}$  phase. This result bounds the utility of isostructural compounds as nucleation particles for salt hydrate phases and illustrates that nucleation strategies relying on isostructural systems are complicated by the solubility relationships and reactivity between the phases present.

Received 15th August 2025,  
Accepted 18th February 2026

DOI: 10.1039/d5ma00906e

rsc.li/materials-advances

## 1. Introduction

Many salt hydrate phase change materials (PCMs) require seeding with nucleation particles to promote reversible solidification with minimal undercooling.<sup>1</sup> Nucleation particles are solid phases that are added to a system to promote nucleation of a desired phase by providing a favorable solid surface to nucleate on. Identification of appropriate nucleation particles for a particular PCM of interest remains an outstanding challenge, relying on relatively qualitative and ill-defined criteria. Generally, nucleation particles that are either epitaxial or isostructural to the crystallizing phase are considered to be favorable candidates, as the similar lattice parameters, space group, and atomic positions allow for a minimization of the difference of interfacial energy between the solid–solid interface between the nucleating surface and the crystallizing phase, thus lowering the energetic barrier to nucleation.<sup>2,3</sup> However, the strategy of selecting isostructural compounds is confounded by the observation that these compounds are often soluble or reactive within each other's melts, which can complicate their long-term stability, and activity as nucleation particles. As a specific example, salt hydrates melt to aqueous brines, which may

induce cation exchange reactions, hydration or dehydration reactions, complete dissolution, or other degradative reaction with other isostructural salt hydrates, all governed by the particular phase relationships in the chemical system. Thus, in support of establishing robust strategies to tailor nucleation particles for particular PCM systems, it is critical to establish chemical criteria which must be satisfied to predict favorable candidate nucleation particles.

Salt hydrate systems are a class of phase change materials (PCMs) that are of interest for potential use in thermal energy storage (TES) systems due to their low cost, high gravimetric and volumetric energy density. However, many salt hydrates tend to exhibit undercooling, a nucleation-limited phenomena where a liquid can cool to a metastable temperature without solidifying. Some examples of salt hydrates that display this behavior include sodium sulfate decahydrate,<sup>2,4,5</sup> sodium acetate trihydrate,<sup>6</sup> calcium chloride hexahydrate,<sup>7,8</sup> magnesium chloride hexahydrate,<sup>1,9</sup> lithium nitrate hexahydrate,<sup>10</sup> and zinc nitrate hexahydrate.<sup>11</sup> In some of these cases, the undercooling is relatively minor and has a minimal effect on the overall system, however, other systems, such as calcium nitrate tetrahydrate, can quench to glassy states very easily.<sup>12</sup> Undercooling is problematic, as it can result in unpredictable solidification, the potential nucleation of and 'trapping' of metastable states, and a lack of reliable behavior of the system, all of which can hinder the utilization of salt hydrates in different thermal energy storage and thermal management applications.

Department of Materials Science and Engineering, Texas A&M University,  
College Station, TX, 77843, USA. E-mail: patrick.shamberger@tamu.edu;  
Tel: +1 979-458-1086



Nucleation particles have been utilized in many different systems to suppress the formation of an undesirable metastable phase by inducing the nucleation of a desired phase. Some of the best known examples, which guided much of the later efforts, include efforts from the 1950's to nucleate ice crystals for cloud seeding,<sup>13,14</sup> and the use of borax (sodium tetraborate decahydrate;  $\text{Na}_2\text{B}_4\text{O}_7 \cdot 10(\text{H}_2\text{O})$ ) as a nucleation particle to nucleate Glauber's salt (sodium sulfate decahydrate;  $\text{Na}_2\text{SO}_4 \cdot 10(\text{H}_2\text{O})$ ), a low cost PCM of interest for building thermal energy storage systems.<sup>2,4</sup> Silver iodide (AgI) is an example of an epitaxial match to ice crystals. Both AgI ( $P6_3mc$ , No. 186) and  $\text{H}_2\text{O}$  ( $P6_3/mmc$ , No. 194) crystallize in hexagonal structures, with similar unit cell volumes and lattice parameters.<sup>15,16</sup> Critically, AgI is mostly insoluble in water, and thus maintains its hexagonal structure in the presence of liquid water, and the (0001) plane of AgI exists, and is able to serve as a template for the basal plane of ice, which decreases the free energy of crystal formation, inducing heterogeneous nucleation to occur.<sup>13,17</sup> As a second example, Glauber's salt (sodium sulfate decahydrate;  $\text{Na}_2\text{SO}_4 \cdot 10(\text{H}_2\text{O})$ ) is a stoichiometric salt hydrate that melts incongruently at 32.35 °C *via* a peritectic reaction.<sup>1</sup> Glauber's salt is nucleated effectively by borax, which is isostructural to the PCM, both being monoclinic (Glauber's salt:  $P2_1/c$  (No. 14) and borax:  $C2/c$  (No. 15)), having similar lattice parameters (within 15% difference), and anions, cations, and water molecules in approximately equivalent positions.<sup>2,18</sup> As an important distinction, while borax is soluble in Glauber's salt at elevated temperatures, borax precipitates out at temperatures exceeding the melting temperature of the PCM, even when present in a small mass fraction relative to the PCM. The precipitation point of borax was determined based on the solubility of sodium sulfate–sodium tetraborate in water by Telkes.<sup>2</sup> Thus, the Glauber's salt - borax pair serves as an informative example, as it demonstrates that a moderate degree of solubility does not exclude a phase from serving as a

nucleation particle, as long as it precipitates in the desired phase above the temperature at which crystallization occurs.<sup>2</sup>

Calcium chloride hexahydrate,  $\text{CaCl}_2 \cdot 6(\text{H}_2\text{O})$  (CCH), is an attractive salt hydrate for use in thermal energy storage applications due to its low melting temperature, high energy density, and low cost (Table 1). However, calcium chloride hexahydrate is prone to undercooling.<sup>7,19</sup> Further complicating matters, stoichiometric  $\text{CaCl}_2 \cdot 6(\text{H}_2\text{O})$  exhibits a peritectic reaction, first transforming to calcium chloride tetrahydrate ( $\text{CaCl}_2 \cdot 4(\text{H}_2\text{O})$ )  $\leftrightarrow \text{CaCl}_2 \cdot 4(\text{H}_2\text{O}) + \text{L}$ , followed by continuous melting until the liquidus temperature is reached (Fig. 1).<sup>20</sup> Of note, melting temperatures determined by differential scanning calorimetry (DSC) are generally defined as the onset of the melting reaction, which represents the peritectic temperature. Comparatively, melting determined by the stable temperature plateau in a larger volume subject to isothermal or slowly heated surroundings, generally represents a combined temperature over which both reactions occur, explaining subtle differences in these reported temperatures (Table 1). During solidification, due to slow diffusion-limited transformation kinetics, residual metastable  $\text{CaCl}_2 \cdot 4(\text{H}_2\text{O})$  can be retained, which over time, could potentially lead to phase segregation and stratification, and thus, can hinder its utilization as a PCM for thermal energy storage. It has previously been observed that the introduction of nucleation particles which favor the hexahydrate over the tetrahydrate, could stabilize the system by preferentially nucleating the hexahydrate or by suppressing the formation of the metastable tetrahydrate phase, reducing the potential for phase segregation.<sup>1,21</sup> An ideal nucleation particle would promote direct nucleation of the hexahydrate phase, bypassing the tetrahydrate phase entirely. Therefore, identifying an active and stable nucleation particle is critical for the long-term utilization of this PCM.

Many different nucleation particles for calcium chloride hexahydrate have been proposed in literature, with a range of

Table 1 Previously reported CCH thermal properties

$T_{\text{fus}}^a$ (°C)	$u_r(T_{\text{fus}})$	$\Delta H_{\text{fusion}}^b$ (J g <sup>-1</sup> )	$u_r(H_{\text{fus}})$	$\Delta T$ (°C)	Method	Ref.	Year
29.2	—	172.5	—	—	Calorimetric testing <sup>c</sup>	22	1977
29.8	—	170	—	<4	Calorimetric testing <sup>c</sup>	23	1979
29.9	—	195	—	—	Melting/freezing testing <sup>d</sup>	24	1984
29	—	201	—	—	Melting/freezing testing <sup>d</sup>	8	1985
29.6	—	190.8	—	—	Calorimetric testing <sup>c</sup>	1	1986
29.8	—	174	—	—	Melting/freezing testing <sup>d</sup> & DSC <sup>e</sup>	25	1988
29	—	—	—	10–25	Melting/freezing testing <sup>d</sup>	7	1992
29.17	—	213.12	—	5	DSC <sup>e</sup>	26	2010
28.4	—	185.6	—	—	DSC <sup>e</sup>	27	2018
28.1–28.8	—	163–199.5	—	~28–38	DSC <sup>e</sup>	28	2019
29.8	0.01	182	0.043	17.2	T-history <sup>f</sup>	19	2019
29.1	—	175	—	—	DSC <sup>e</sup>	29	2019

<sup>a</sup>  $T_{\text{fus}}$ : here  $T_{\text{fus}}$  is generally defined as the onset of the melting reaction, which represents the peritectic temperature, whereas  $T_{\text{fus}}$  in a melting/freezing test or a T-history test refers to a stable plateau temperature, which lumps both melting at the peritectic point and when the system reaches the liquidus temperature. <sup>b</sup>  $\Delta H_{\text{fus}}$ : here  $\Delta H_{\text{fus}}$  in all methods described is generally unable to discriminate between a peritectic reaction and melting of the tetrahydrate phase along its liquidus, due to the narrow temperature range of these two processes. Thus,  $\Delta H_{\text{fus}}$  represents the combined enthalpy difference between CCH and the liquid phase. <sup>c</sup> Calorimetric testing: determined by unspecified form of calorimetry. <sup>d</sup> Melting/freezing testing: larger scale testing (80–700 g), slower continuous heating and cooling rates (10–20 °C h<sup>-1</sup>), temperature measured *via* thermocouple. <sup>e</sup> DSC: differential scanning calorimetry, small sample size (10–20 mg), continuous heating and cooling at fast rates (7 °C min<sup>-1</sup>), temperature measured by DSC system. <sup>f</sup> T-history: (~10 to 15 mL) sample was heated and cooled between 24–40 °C by free convection in an environmental chamber, and temperature of the system was measured *via* thermocouple.



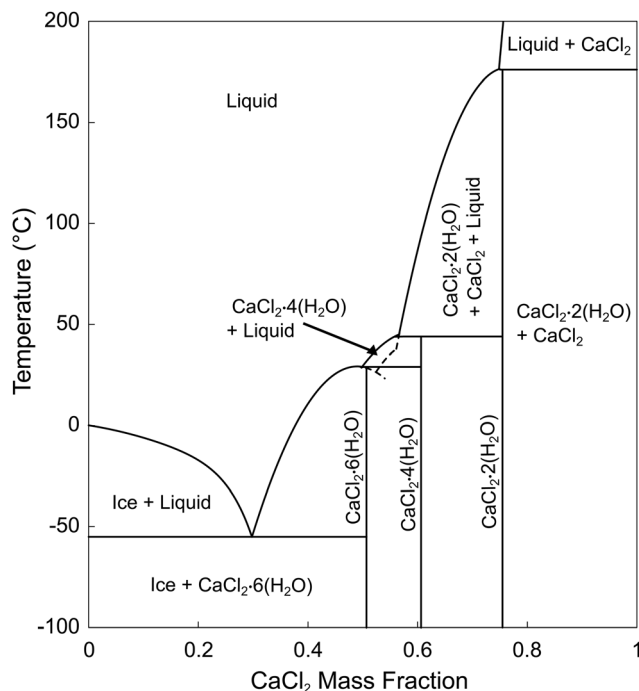


Fig. 1 Calcium chloride - water phase diagram, adapted with permission from Schmit, *et al.*<sup>30</sup> based on equations from Conde, *et al.*<sup>31</sup>

structural relationships to calcium chloride hexahydrate, including an isostructural match (strontium chloride hexahydrate) and nucleation particles with no apparent structural match (barium based compounds: barium carbonate, barium hydroxide, barium hydroxide octahydrate, *etc.*).<sup>7,32</sup> Strontium chloride hexahydrate,  $\text{SrCl}_2 \cdot 6(\text{H}_2\text{O})$  (SCH), is a stoichiometric salt hydrate that is often cited as an effective nucleation particle for CCH, premised on the fact that SCH is an isostructural crystallographic match to CCH (Table 2). However, SCH's use as a nucleation particle has been questioned in multiple studies, resulting in confusion in the literature (Table 3). Furthermore, it has been observed that strontium chloride hexahydrate is reactive in calcium chloride hexahydrate under certain ranges of relative concentration and temperature, which could also affect the activity of the nucleation particle. Several studies have noted that the activity of strontium chloride hexahydrate has a time dependence.<sup>7,23,33</sup> Based on the established  $\text{CaCl}_2$ - $\text{SrCl}_2$ - $\text{H}_2\text{O}$  phase diagrams (Fig. 2), strontium chloride hexahydrate and calcium chloride hexahydrate are not in equilibrium with each other for less than 16 wt% SCH over the temperature range 29 to 60 °C, explaining previous observations that the activity of SCH degrades with time.<sup>34</sup>

In this study, we evaluated the activity and stability of strontium chloride hexahydrate as an isostructural nucleation

particle for calcium chloride hexahydrate to determine the required conditions for an isostructural nucleation particle to be effective. We observed both a time and temperature dependent effect on the undercooling of CCH after addition of SCH. SCH can effectively nucleate CCH immediately after its introduction, but after a critical period of time, the activity of SCH is lost. However, we also observed that it was possible to recover the activity of the SCH as a nucleation particle (1) by supercooling the system and holding it at a low temperature for a period of time to induce crystallization of the strontium chloride hexahydrate phase, or (2) by dramatically increasing the relative concentration of SCH. Given these observations, we hypothesize that while SCH is isostructural to CCH, it does not satisfy the critical constraint that the desired nucleation particle phase must be in equilibrium with the solid at  $T > T_{\text{fus}}$  at low concentrations of the nucleation particle phase. Thus, this study clarifies the previously described behavior of nucleation in CCH/SCH mixtures and provides an informative example of the limitations on selecting isostructural nucleation particles as effective nucleation particles for salt hydrate systems.

## 2. Methods

### 2.1. Materials

Calcium chloride hexahydrate (CCH),  $\text{CaCl}_2 \cdot 6(\text{H}_2\text{O})$ , (crystallized, >99.0%) was obtained from Sigma Aldrich, and was used as received (Fig. S1). Strontium chloride hexahydrate (SCH),  $\text{SrCl}_2 \cdot 6(\text{H}_2\text{O})$ , (crystallized, 99–103% ACS) was obtained from Beantown Chemical, and was also used as received. SCH was observed to be dominated by the single hexahydrate phase, within the resolution of the XRD experiment (XRD presented in results section, Fig. 7), but CCH was too hygroscopic to collect a satisfactory pattern using available facilities. However, based on the XRD spectra, there may be trace amounts of the strontium chloride dihydrate phase present, as evidenced by a small peak around  $2\theta = 15^\circ$ . Both melting points and enthalpies of fusion of both compounds, as measured by differential scanning calorimetry (DSC), were consistent with previously reported values (Fig. 3 and Table 1). No additional melting peaks were observed which would be expected with additional hydrate phases (*e.g.*, tetrahydrate or dihydrate) present. Additionally, thermogravimetric analysis (TGA) was run on neat CCH, with a temperature range of approximately 24 °C to 300 °C with a ramp rate of 5 °C  $\text{min}^{-1}$ . Three samples of approximately  $9.0 \pm 1.3$  mg each of CCH were tested and were observed to have an average mass loss of  $(48.2 \pm 2.1)\%$ , which is within uncertainty of the theoretical mass loss of complete dehydration of CCH of 49.3% (Fig. S2).

Table 2 Literature reported crystallographic overview

	Space group	$[a, b, c]$ (Å)	$[\alpha, \beta, \gamma]$ (°)	Ref.
$\text{CaCl}_2 \cdot 6(\text{H}_2\text{O})$	<i>P</i> 321 (No. 150)	[7.876, 7.876, 3.954]	[90, 90, 120]	7 and 35
$\text{SrCl}_2 \cdot 6(\text{H}_2\text{O})$	<i>P</i> 321 (No. 150)	[7.94, 7.94, 4.11]	[90, 90, 120]	7 and 35–37
$\text{SrCl}_2 \cdot 2(\text{H}_2\text{O})$	<i>C</i> 12/ <i>c</i> 1 (No. 15)	[11.71, 6.39, 6.67]	[90, 105.7, 90]	36



Table 3 Prior studies which reported using SrCl<sub>2</sub>·6(H<sub>2</sub>O) as a nucleation particle for CCH

System composition	Conc. SCH (wt%)	$T_{\text{fus}}$ (°C)	$\Delta H_{\text{fus}}$ (J g <sup>-1</sup> )	$\Delta T$ (°C)	Testing parameters	Cooling ramp rate (°C min <sup>-1</sup> )	Ref.	Year
Observed decrease in undercooling								
CCH + SCH + SiO <sub>2</sub>	2	28	71	1.8	15–45 °C range, heating rate = 0.5 °C min <sup>-1</sup> .	0.33	8	1985
CCH + SCH	3	—	—	~1.0	Cycled between 18–40 °C.	—	38	1989
CCH + MgCH <sup>a</sup> + SCH/SrCO <sub>3</sub>	3	21.4	102.3	2	DSC	—	39	2014
+ hydroxyethyl cellulose (HEC)								
CCH + SCH + KNO <sub>3</sub> + KBr	0	21.4	203.3	15.5	DSC - Cycled between 0–40 °C	1.0	40	2015
	0.5			2.7	with N <sub>2</sub> flow & thermal cycling tests.			
	1			1.5				
	2			0.4				
	3			1.8				
CCH + SCH + C <sub>5</sub> H <sub>14</sub> ClNO	0.5	20.65–24.10	±2	<2.54	DSC: heating rate of	—	41	2016
+ hydroxymethyl cellulose + SiO <sub>2</sub>	1				1 °C min <sup>-1</sup>			
	2							
CCH + SCH + graphene oxide	0.2	35.2	206.4	21.0	DSC, thermal cycling	1.0	42	2017
	0.5		—	18.6	(1 °C min <sup>-1</sup> )			
	0.8		207.9	6.0				
CCH + SCH + methyl cellulose	2	11.62	127.2	0.95	50 heating/cooling cycles.	—	43	2018
+ CH <sub>4</sub> N <sub>2</sub> O + C <sub>2</sub> H <sub>5</sub> OH								
CCH + SCH	1	30.5	181.3	2	DSC (–30 °C to 50 °C),	7.0	28	2019
	3	29.2	171.5		thermal cycling			
	5	29.6	165					
CCH + SCH	1	29.6 ± 0.16	182 ± 8	2.5 ± 0.5	1000 melt-freeze cycles	—	19	2019
	2				(T-history measurement range: 24–40 °C)			
	3							
CCH + SCH + MgCH <sup>a</sup>	5	23	130	0.7	100 cycles	—	44	2021
CCH + SCH + NaCl or KCl	2			0	—	—	45	2022
CCH + SCH + CH <sub>4</sub> N <sub>2</sub> O + NH <sub>4</sub> Cl	1–2	9.52	99.56	0.94	DSC: –20 to 30 °C.	5.0	46	2023
CCH + SCH + cellulose nanofibril	3	32.93	181.28	2.07	DSC: –40 °C to 50 °C.	5.0	47	2024
Observed no change in undercooling								
CCH + SCH + oxidation expandable graphite	3	27.6–29.6	172.26	0–1.4	DSC: under Argon	1.0	48	2016
Observed that the SCH activity had a time dependence								
CCH + SCH	<3	—	—	Lowered in some cases	Cycled between 22–35 °C, cycle period = 1 day.	—	33	1984
CCH + SCH	0.1	—	9.4	0–9.4	Sample of ~80 g was prepared and heated to >10 °C above $T_{\text{fus}}$ and allowed to cool, 11–15 cycles.	—	7	1992
	0.5		6.2					
	1		0					
CCH + SCH	2	—	169 ± 5	3	—	—	23	1979

<sup>a</sup> MgCH = MgCl<sub>2</sub>·6(H<sub>2</sub>O).

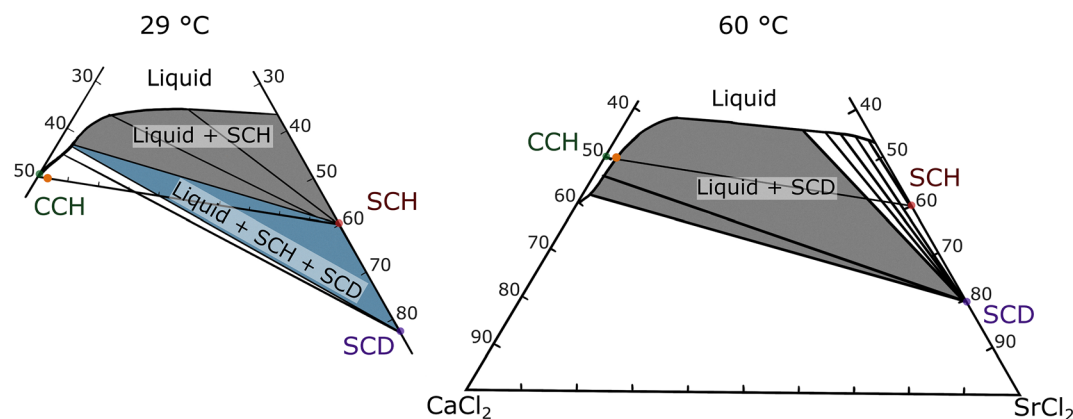


Fig. 2 Ternary phase diagram of CaCl<sub>2</sub>–SrCl<sub>2</sub>–H<sub>2</sub>O chemical system at 29 °C and at 60 °C, adapted with permission from Assarsson 1953.<sup>34</sup> SCH refers to SrCl<sub>2</sub>·6(H<sub>2</sub>O) and SCD refers to SrCl<sub>2</sub>·2(H<sub>2</sub>O). The orange dot on both phase diagrams refers to the average composition used for DSC testing (approximately 2 wt% SCH immersed in a volume of CCH).



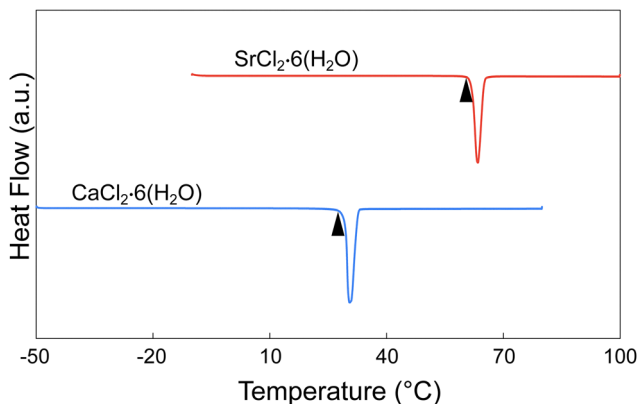


Fig. 3 DSC of neat calcium chloride hexahydrate ( $T_{\text{fus}} = 28.5\text{ }^{\circ}\text{C}$  and  $\Delta H_{\text{fus}} = 187.7\text{ J g}^{-1}$ ) and neat strontium chloride hexahydrate ( $T_{\text{fus}} = 62.0\text{ }^{\circ}\text{C}$  and  $\Delta H_{\text{fus}} = 158.1\text{ J g}^{-1}$ ) with heating and cooling ramp rates of  $1\text{ }^{\circ}\text{C min}^{-1}$  prepared and hermetically sealed under an inert nitrogen environment.

## 2.2. X-ray diffraction

A Bruker-AXS Advanced Bragg–Brentano X-ray Powder Diffractometer was used to collect wide-angle diffraction spectra. The X-ray source was a 2.2 kW Cu X-ray tube, maintained at an operating current of 40 kV and 25 mA. The X-ray optics was the standard Bragg–Brentano *para*-focusing mode with a position sensitive X-ray Detector (Lynx-Eye, Bruker-AXS). The two-circle 250 mm diameter goniometer was computer controlled with independent stepper motors and optical encoders for the theta and  $2\theta$  circles with the smallest angular step size of 0.0001 degrees  $2\theta$ . The resulting XRD spectra was refined using GSAS-II.<sup>49</sup> XRD was used to verify the composition of the SCH, in the ‘before’ case, the SCH was tested as-received from the manufacturer, and in the ‘after’ case, the SCH was tested after being in solution with liquid CCH at an elevated temperature for a period of time. However, due to the structural similarities between SCH and CCH, chemically separating the insoluble particulate from CCH was not possible. Therefore, the insoluble particles within the CCH were physically removed and excess liquid CCH was absorbed off the particulate, before running the sample in the XRD.

## 2.3. Differential scanning calorimetry

To analyze SCH as a nucleation particle for CCH, differing weight percentages of strontium chloride hexahydrate were mixed with stoichiometric calcium chloride hexahydrate before analysis. Samples of calcium chloride hexahydrate with strontium chloride hexahydrate were prepared to assess the melting temperature ( $T_{\text{fus}}$ ), the heat of fusion ( $\Delta H_{\text{fus}}$ ) of the phase change, and the crystallization temperature ( $T_{\text{crys}}$ ) of the system. As these materials have peritectic reactions, the melting temperature ( $T_{\text{fus}}$ ) refers to the peritectic temperature ( $T_{\text{peritectic}}$ ) and the heat of fusion ( $\Delta H_{\text{fus}}$ ) represents a lumped measure of the enthalpy evolved due to both the peritectic reaction and to the melting of either the tetrahydrate or residual hexahydrate phases. All samples were sealed in Tzero aluminum pans with hermetic lids (TA Instruments) to mitigate water loss or

absorption to the environment. The average mass of a DSC sample was  $10.7 \pm 1.0\text{ mg}$ , and thus no effects from variation in sample masses were expected or observed (Fig. S3). Within an approximate 120 hour time span, three DSC samples were observed to have, on average, a  $-0.04 \pm 0.03\text{ mg}$  mass change, supporting the claim that negligible quantities of water entered or left the DSC pan after hermetically sealing. A TA Instruments Q2000 differential scanning calorimeter (DSC) was used. The Q2000 calorimeter was calibrated with a pure indium standard ( $w = 0.9999$ ), using reference values of  $T_{\text{fus}} = 156.598\text{ }^{\circ}\text{C}$  and  $\Delta H_{\text{fus}} = 28.662\text{ J g}^{-1}$ , and with a pure tin standard ( $w = 0.9999$ ), with reference values of  $T_{\text{fus}} = 231.9\text{ }^{\circ}\text{C}$  and  $\Delta H_{\text{fus}} = 60.216\text{ J g}^{-1}$ .<sup>50,51</sup> The relative uncertainties ( $u_r$ ) for individual measurements at a 95% confidence interval, is based on repeated analysis of the previously mentioned standards for the Q2000 are  $u_r(T_{\text{fus}}) = \pm 0.0027$  and  $u_r(\Delta H_{\text{fus}}) = \pm 0.0095$  for indium, and  $u_r(T_{\text{fus}}) = \pm 0.00017$  and  $u_r(\Delta H_{\text{fus}}) = \pm 0.0023$  for tin. Any deviations between reported sample averages and reference values for the Q2000,  $\delta = \frac{X_{\text{obs}} - X_{\text{ref}}}{X_{\text{ref}}}$ , are within  $\pm 0.0038$  and  $\pm 0.0419$  for  $T_{\text{fus}}$  and  $\Delta H_{\text{fus}}$ , respectively.<sup>52</sup> All samples were initially subjected to heating and cooling cycles at a rate of  $10\text{ }^{\circ}\text{C min}^{-1}$  over the range  $T_{\text{fus}} \pm 50\text{ }^{\circ}\text{C}$  with a continuous nitrogen flow of  $50\text{ cm}^3\text{ min}^{-1}$ . Following the standard DSC techniques (ASTM E793-06), the melting peak onset was reported as  $T_{\text{fus}}$ , and is defined by the intercept of a linear baseline with the maximum slope tangent to the melting curve. Undercooling ( $\Delta T$ ) is defined as the difference between the melting temperature and the solidification (crystallization) temperature ( $\Delta T = T_{\text{fus}} - T_{\text{crys}}$ ), with  $T_{\text{crys}}$  defined by the onset of the abrupt exothermic crystallization peak.  $\Delta H_{\text{fus}}$ , the heat of fusion, is determined through the integration of the melting peak.

## 3. Results/discussion

### 3.1. The impact of reaction kinetics on measurement of nucleation behavior

When solid strontium chloride hexahydrate powder is introduced into liquid calcium chloride hexahydrate, strontium chloride hexahydrate only actively promotes nucleation of CCH below certain temperatures and for short periods of time. This behavior suggests that SCH is only kinetically metastable; given sufficient time for SCH to equilibrate with the host liquid CCH, the hexahydrate phase SCH is no longer present. In Fig. 4, the sample was prepared by adding approximately 2 wt% of strontium chloride hexahydrate to calcium chloride hexahydrate immediately before running the sample in the DSC. The sample was subjected to multiple cooling and heating cycles, with an increasing  $T_{\text{max}}$  each cycle (first cycle  $T_{\text{max}} = 45\text{ }^{\circ}\text{C}$ , and increased by  $5\text{ }^{\circ}\text{C}$  increments, ending at a  $T_{\text{max}} = 80\text{ }^{\circ}\text{C}$ , with a 2-minute hold at each maximum temperature). During the cycles with a  $T_{\text{max}}$  of  $45\text{--}60\text{ }^{\circ}\text{C}$ , the undercooling was around  $\sim 10\text{ }^{\circ}\text{C}$ , however, once the  $T_{\text{max}}$  exceeded  $60\text{ }^{\circ}\text{C}$  (with a 2-minute hold at the maximum temperature), the observed undercooling began to greatly increase. This indicated that,



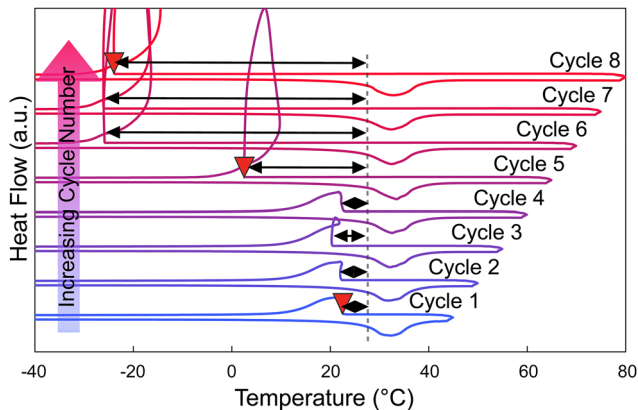


Fig. 4 Uninterrupted DSC Cycling of a single sample of CCH containing approximately 2 to 4 wt% SCH, with  $T_{\max}$  increasing each cycle ( $T_{\max} = 45, 50, 55, 60, 65, 70, 75, 80$  °C) and  $T_{\min} = -50$  °C. Sample was prepared immediately prior to DSC testing. The grey dashed line represents the approximate onset of melting of each cycle ( $T_{\text{fus}}$ ). The downward-pointing triangles in the figure represent the onset of crystallization ( $T_{\text{crys}}$ ) in select cycles. The double headed arrows on each cycle indicate the undercooling ( $\Delta T = T_{\text{fus}} - T_{\text{crys}}$ ).

for this combination of equilibration temperature and time, the strontium chloride hexahydrate has likely reacted and changed its hydration state. Notably, there is no direct observation of a heat of dehydration in the DSC experiment, likely due to the facts that: (1) this reaction is slow and extended over time (or over temperature in a scanning DSC experiment), (2) the total mass of SCH in DSC pans are  $< 0.5$  mg, which is too small of a mass to reliably measure a signal for, and (3) the enthalpy associated with the dehydration reaction is unknown, but it may also be small. It was also observed that time spent at an elevated temperature impacts the measured nucleation rate in the supercooled system, consistent with the observation that the reaction rate of this reaction impacts nucleation behavior in calorimetry experiments. For Fig. 5, a sample of CCH to which we added 2–4 wt% of SCH was cycled from  $-50$  °C to  $60$  °C, with isothermal holds at  $60$  °C for increasing amounts of time (2-, 5-,

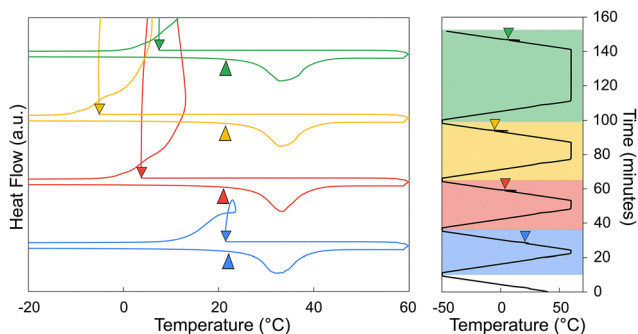


Fig. 5 Uninterrupted DSC cycling of a single sample of CCH containing approximately 2 to 4 wt% SCH, with  $T_{\max} = 60$  °C and  $T_{\min} = -50$  °C, with 2, 5, 10, 30-minute holds at  $T_{\max}$  (60 °C). Sample was prepared immediately prior to DSC testing. The upwards-pointing arrows represent the approximate onset of melting ( $T_{\text{fus}}$ ), and the downward-pointing arrows represent the onset of crystallization ( $T_{\text{crys}}$ ).

10-, and 30-minutes holds). From this experiment, it was observed that when the sample was held at an elevated temperature for a longer period of time ( $> 5$  minutes), SCH began to lose activity as a nucleation particle, as indicated by the increase in undercooling.

These experiments are all consistent with the previously reported equilibrium data which indicates that under all temperatures above the melting point, small concentrations of strontium chloride hexahydrate (SCH) are not stable in the presence of CCH solution, reacting to the dihydrate phase (SCD; Fig. 2). We infer from our DSC experiments that the kinetics of this reaction rate are somewhat sluggish, and not directly observable until the system has been super-heated above approximately  $60$  °C, or has been held for long enough time to fully equilibrate. The sluggish reaction rate, in our view, explains much of the previous confusion in the literature (Table 3) on the efficacy of SCH as a nucleation particle for CCH. Finally, it should be acknowledged that at small mass fractions (2–4 wt% of SCH), complete dissolution of a solid strontium chloride phase is also possible, especially at higher temperatures ( $> 60$  °C), although lower hydrate phases would still likely reprecipitate once the solution was cooled below  $60$  °C, upon the cooling leg.

### 3.2. Stabilization of strontium chloride hexahydrate at higher concentrations

To evaluate the effect of composition on the reactivity of SCH, multiple samples with differing amounts of calcium chloride hexahydrate (100 to 67 wt%) and strontium chloride hexahydrate (0 to 33 wt%) were evaluated by repeatedly cycling each sample in the DSC (Fig. 6). Previous experimental work (Fig. 2<sup>34</sup>) indicated that at lower temperatures, SCH was stabilized relative to SCD. However, this data does not extend to temperatures below room temperature. Therefore, to evaluate the hypothesis that at sufficiently high concentrations, SCH will remain present after thermal cycling and will be available to promote the nucleation of CCH, cycling testing was performed to evaluate the reaction kinetics and the effects of thermal path on the system undercooling. For each cycle, the sample was first cooled to  $-50$  °C; for the first cycle, the maximum temperature was  $60$  °C, the second cycle had a maximum temperature of  $80$  °C, and in the last cycle, the system was held at  $0$  °C for 15 minutes before heating up to  $60$  °C.

Even at higher concentrations of SCH, when exposed to higher temperatures for longer periods of time, SCH will react to SCD. However, even at those higher concentrations, the mixture of CCH + SCH is also observed to recover its ability to decrease undercooling in CCH after cooling the system to low temperatures ( $-50$  °C), even after thermally cycling up to  $60$  °C for short periods of time. Previous equilibrium data (only available for the temperature range  $18$  °C to  $100$  °C) indicates a minimum concentration of 40 wt% SCH required for the strontium chloride hexahydrate phase to be in equilibrium with CCH at  $29$  °C (Fig. 2). However, equilibrium data is notably absent for temperatures below the melting point of CCH. From this series of experiments, we conclude: (i) at SCH



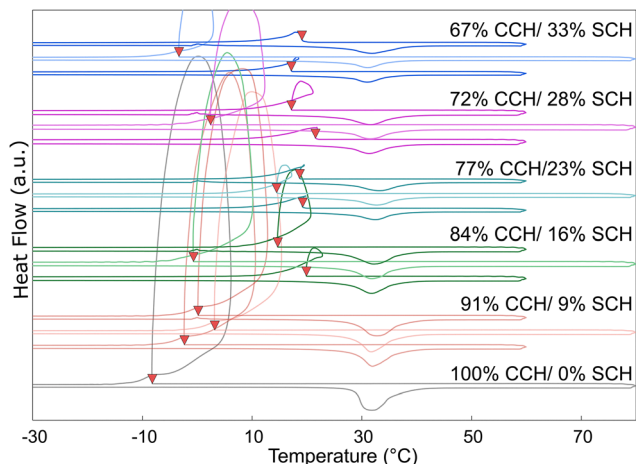


**Fig. 6** Reactivity of SCH in CCH (DSC) cycling of multiple samples, each sample was a mix of strontium chloride hexahydrate and calcium chloride hexahydrate, with increasing SCH wt% (each sample was heated and cooled at  $1\text{ }^{\circ}\text{C min}^{-1}$ ). In the first cycle, the sample was heated to a  $T_{\text{max}}$  of  $60\text{ }^{\circ}\text{C}$  and held there for 2 minutes, after, the sample was then cooled to  $-50\text{ }^{\circ}\text{C}$  with a 2-minute hold. In the second cycle, the sample was then heated to  $80\text{ }^{\circ}\text{C}$ , held for 2 minutes, and then cooled back down to  $-50\text{ }^{\circ}\text{C}$  with a 2-minute hold. For the last cycle, the sample was heated to  $0\text{ }^{\circ}\text{C}$  and then held there for 15 minutes, and then heating continued to  $60\text{ }^{\circ}\text{C}$  with a 2-minute hold, and the sample was then cooled back down to  $-50\text{ }^{\circ}\text{C}$ .

concentrations as low as 16 wt%, the efficacy of SCH to decrease the undercooling in CCH is recovered, implying the re-emergence of the strontium chloride hexahydrate phase at low temperatures which promotes nucleation of CCH. Furthermore, (ii) upon melting and heating to  $60\text{ }^{\circ}\text{C}$ , the undercooling in CCH remains small, which is likely attributable to kinetic effect due to the sluggish reaction rate of the dehydration reaction. Finally, (iii) thermally cycling to  $80\text{ }^{\circ}\text{C}$  generally resulted in large undercooling on the subsequent cooling experiment, suggesting that this heating cycle was sufficient (in most cases) to complete the reaction of strontium chloride

hexahydrate to strontium chloride dihydrate, thereby losing the ability of the system to nucleate at small undercooling extents in the subsequent cooling cycle.

To further support these indirect inferences of reactions between strontium chloride hexahydrate and strontium chloride dihydrate phases with direct observations of the phases present in the system after equilibration, a larger volume (approximately 10 mL) sample of 60 wt% CCH/40 wt% SCH was synthesized and was equilibrated at  $40\text{ }^{\circ}\text{C}$  for a period of 13 months. Equilibrium data suggests that these conditions should result in near complete reaction of strontium chloride hexahydrate to strontium chloride dihydrate (Fig. 2). After equilibration, approximately 0.2 g of residual solid was separated from the liquid (which will be referred to as “reacted NP”). XRD analysis on the “reacted NP” revealed that the residual solids had partially reacted to the dihydrate phase, although this reaction was incomplete (Fig. 7); the dominant phase present in the diffraction spectra was strontium chloride dihydrate, accompanied by some residual strontium chloride hexahydrate. Quantitative analysis of phase abundance proved impossible, likely due to larger grain size and poor statistical sampling of the recovered solids. We infer that the residual hexahydrate phase may reflect either: (1) internal particle volumes which did not react due to diffusion limitations, or (2) some re-conversion of the dihydrate phase to the hexahydrate phase during separation of the solid particles and subsequent analysis by XRD (which occurred open to the environment). A similar test was completed with a lower concentration of SCH (5 wt% SCH/95 wt% CCH) which was equilibrated at  $30\text{ }^{\circ}\text{C}$  for a period of approximately 1 week, and the XRD spectra of the reacted material showed a similar result, exhibiting the signature of both SCH and SCD phases present in the XRD spectra (Fig. S4). Therefore, at temperatures higher than the melting point of the system ( $\sim 29\text{ }^{\circ}\text{C}$ ), there is a tendency for the SCH to react to SCD, even with differing concentrations of SCH initially present in the sample.

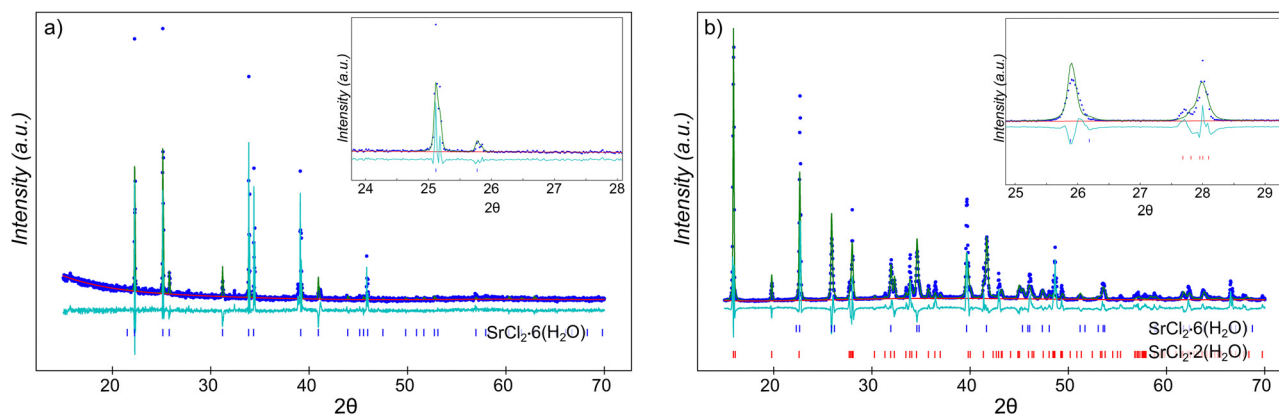


**Fig. 7** Refined powder diffraction data for: (a) as-received strontium chloride hexahydrate, that matches well to the calculated powder pattern for strontium chloride hexahydrate (100 wt%  $\text{SrCl}_2\cdot 6(\text{H}_2\text{O})$ ,  $R_{\text{wp}} = 25.04$ , reduced  $\chi^2 = 5.99$ ), and (b) reacted strontium chloride hexahydrate. This sample was equilibrated at  $40\text{ }^{\circ}\text{C}$  for a period of approximately 13 months, at a concentration of (40 wt% SCH/60 wt% CCH). The reacted sample is consistent with the presence of both strontium chloride hexahydrate and strontium chloride dihydrate ( $R_{\text{wp}} = 28.27$ , reduced  $\chi^2 = 25.37$ ). The quality of Rietveld refinements were limited by the poor sampling statistics due to relatively large grain sizes.



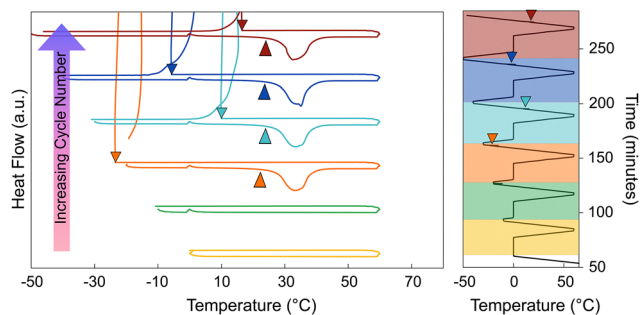


**Fig. 8** Uninterrupted DSC cycling of a single sample of CCH containing approximately 2–4 wt% SCH, that was subjected to a pre-melt cycle with a  $T_{\max}$  of 80 °C, and then cycled to different  $T_{\min}$  (0, –10, –20, –30, –40, –50), with a hold each cycle at 0 °C for 15 minutes. The upwards-pointing arrows represent the approximate onset of melting ( $T_{\text{melt}}$ ), and the downward-pointing arrows represent the onset of crystallization ( $T_{\text{cryst}}$ ).

This direct observation supports our hypothesis that upon heating, even at higher concentrations of SCH initially, SCH will eventually react to SCD.

### 3.3. Recovery of effective strontium chloride hexahydrate phase

Nucleation particle activity was recovered after the system was cooled and held at a low temperature (at –30 °C for at least 5 minutes). In Fig. 8, the sample was prepared by adding approximately 2 wt% of strontium chloride hexahydrate to calcium chloride hexahydrate immediately before running the sample in the DSC. The sample was first subjected to a pre-melt cycle ( $T_{\max} = 80$  °C), after which it was subjected to multiple heating and cooling cycles, with a decreasing minimum temperature each cycle and with an isothermal hold at 0 °C for 10 minutes each cycle. When the CCH/SCH system was cooled sufficiently (below approx. –30 °C) and held at a low temperature for a few minutes (a minimum of 5 minutes), the degree of undercooling began to decrease, indicating that strontium

chloride hexahydrate has regained its activity as a nucleation particle. We hypothesize that this recovery of activity, by cooling to and holding at a low temperature, is an equilibrium process, allowing the SCH phase to reform within the system.

The ability to recover the nucleation particle activity was also tested over subsequent cycling (Fig. 9), suggesting that it was generally possible to repeatedly recover the nucleation particle for 10 cycles. In this experiment, each cycle included melting and heating to 80 °C, where it has been observed that SCH loses activity as a nucleation particle. After melting, the system was cooled down to –35 °C and then held at 0 °C for 10 minutes (Fig. S5). By cooling the system to a low temperature for an extended period, the system was generally able to recover the more stable strontium chloride hexahydrate phase at lower temperatures, resulting in a decrease of measured undercooling during the subsequent solidification of CCH. Thus, in this limited cycling experiment, the undercooling was observed to decrease after almost every low temperature hold. Notably, in cycles 8 and 9, undercooling did not decrease after the low temperature hold. We attribute this inconsistency to: (i) the somewhat stochastic nature of the SCD to SCH reaction, which may not proceed to equal extents in each experiment, (ii) the potential evolution of particle size and shape during each cycle, and (iii) variation in the microstructure of surface defects of the resulting SCH, which may impact its ability to nucleate CCH. Nevertheless, the key observation here is that this process appears generally repeatable. We expect that scaling to larger volumes would only help make this system more reversible, given the larger potential surface area to promote nucleation.

In previous studies, phase diagrams were only established down to a minimum temperature of 18 °C.<sup>34</sup> However, based on our work, the re-establishment of low undercooling after the CCH/SCH system has been cooled down to a low temperature (below approx. –30 °C) and held there for a few minutes (5 minutes) was inferred to reveal the re-occurrence of SCH. Thus, we hypothesize that at low temperatures, a stable mixture

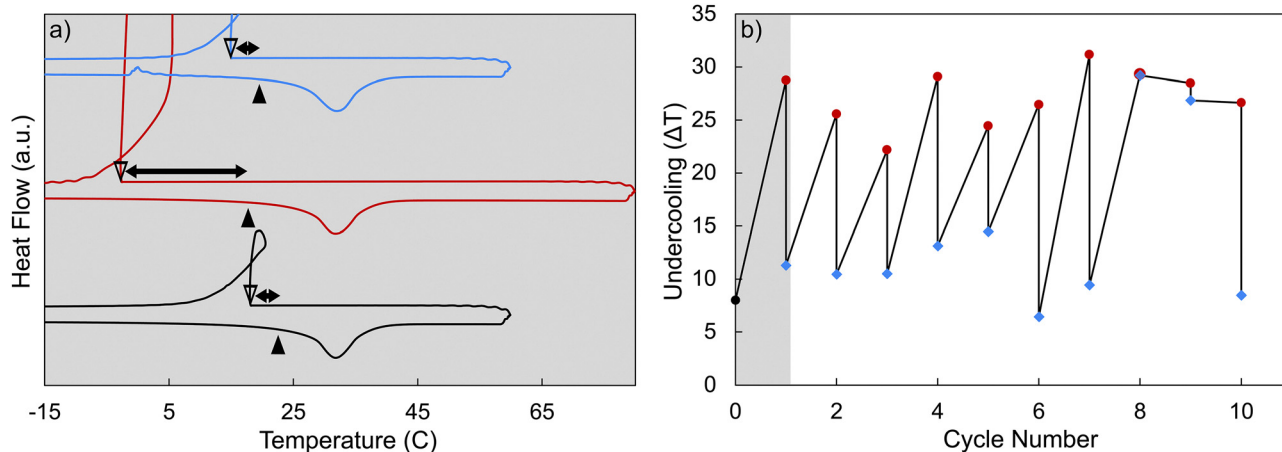


**Fig. 9** Uninterrupted DSC cycling of a single sample of CCH containing approximately 5 wt% SCH: (a) cycling (DSC) from –35 to 80 °C (cycled a total of 10 times – 1st cycle includes both the red (1st) and blue (2nd) DSC curves, where black curve is a time 0 test of the material), with a hold at 0 °C for 10 minutes, and (b) shows the undercooling of each cycle over time. Uncertainty on the reported undercooling, and thus the onset temperatures of each nucleation and melting event, is smaller than the symbol size.



of strontium chloride hexahydrate and calcium chloride hexahydrate is reformed. Therefore, with the effective NP phase then recovered and present in solution, the undercooling of the system was decreased.

### 3.4. Strategies for evaluating the activity of isostructural nucleation particles

As a robust, well understood case, the Glauber's salt/borax system fulfills both of the key criteria for an isostructural nucleation particle to be effective: (1) the lattice parameters of the NP must be sufficiently similar to the crystallizing material with an appropriately close match, and (2) the NP is must be in equilibrium with the crystallizing material at some temperature above  $T_{\text{fus}}$ . Based on the two required conditions for an isostructural nucleation particle, strontium chloride hexahydrate does not uphold both conditions. Because SCH reacts with the CCH, the active SCH phase is not always present in solution, and thus, the isostructural SCH phase is not in equilibrium with the CCH phase at temperatures above the melting temperature (Fig. 10). While it is possible to recover the activity of SCH, either by subcooling the system or by adding greater than 16 wt% of SCH to the system, both recovery

methods do add complexity to the system design, but in some cases may be an effective option.

## 4. Conclusions

In this study, we observed that for calcium chloride hexahydrate and strontium chloride hexahydrate, an isostructural system, the nucleation pathways are not as straightforward as previously believed due to tendency of the nucleation particle (SCH) to react with the salt hydrate PCM in its liquid state. As strontium chloride hexahydrate will react to a lower hydrate state in calcium chloride hexahydrate, the effective nucleating phase—the strontium chloride hexahydrate—will no longer be present in solution and thus will not be effective. Therefore, practical use of SCH as a NP in CCH is impeded by the observation that the system would need to be subcooled by a great amount each cycle to retain activity of the SCH. This process would be impractical for most TES applications. Alternatively, the activity of SCH could also be maintained by adding large amounts ( $\geq 16$  wt%) of SCH to the system. Adding  $\geq 16$  wt% SCH will reduce the energy density of CCH from  $187.7 \text{ J g}^{-1}$  (the neat system) to approximately  $156.6 \text{ J g}^{-1}$ , and thus the trade-off between nucleation effect and energy density will need to be considered. Cooling at  $-30 \text{ }^\circ\text{C}$  will require additional cooling energy consumption but could be suitable for intermittent energy storage systems (for example, cooling with off-peak electricity at night). However, as both of those methods will add complexity to the system design, practical applications will likely favor other nucleation particles for CCH, for example, several barium-based compounds have been determined to be effective nucleation particles for CCH. Despite the lack of structural relationship with CCH, many barium-based nucleation particles are effective NPs for CCH, as the activity of barium-based NPs is likely due to atomic scale defects on the surface of a solid solution phase. These defects allow the barium-based NPs to be effective nucleators for CCH for extended periods of time.<sup>7,32</sup>

The results presented here allow us to further assess the claim that the introduction of nucleation particles could stabilize CCH (over the metastable calcium chloride tetrahydrate phase) by preferentially nucleating the hexahydrate or by suppressing the formation of the metastable tetrahydrate phase, thereby reducing the potential for phase segregation.<sup>1,21</sup> The inference underlying this claim is that decreasing the kinetic barrier to form one of these phases by introducing a phase selective nucleation particle functionally increases the probability of nucleation and therefore solidification of the desired hexahydrate phase. However, if the nucleation particle reacts to a form that no longer actively promotes nucleation of CCH, it will no longer serve its function to “stabilize” CCH. Furthermore, the effect of other strategies that may be adopted to stabilize the hexahydrate phase (*e.g.*, operating under a slightly water-rich composition) can be evaluated by considering the phase relationships represented in Fig. 2. That is, even for systems with slightly excess water (*i.e.*, that do not sit directly

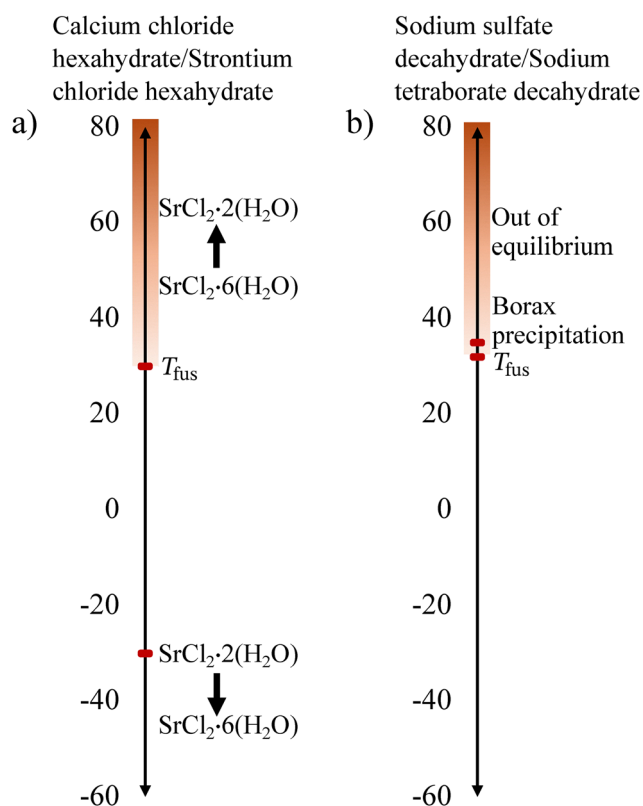


Fig. 10 (a) CCH/SCH system versus (b) Glauber's salt/borax system, showing at which temperatures thermal behavior/events occur. The SCH recovery point is the maximum temperature required for the system to be able to recover the strontium chloride hexahydrate phase for a system with approximately 2–10 wt% of SCH. The borax precipitation point was determined based on the solubility of sodium sulfate–sodium tetraborate in water, and based on a system with approximately 2 wt% of borax in Glauber's salt.<sup>2</sup>



on the mixture line between CCH and SCH), SCH is not a stable phase. Thus, we would anticipate that SCH is not a stable phase in a water rich system, and observed undercooling would follow similar behavior to that presented in this manuscript.

In summary, this investigation into the calcium chloride hexahydrate/strontium chloride hexahydrate system reveals the two conditions that must be upheld for an isostructural nucleation particle to be effective: (1) the lattice parameters must be sufficiently similar in order to nucleate the host phase and (2) the isostructural phase must be in equilibrium with the solid at  $T > T_{\text{fus}}$ . Therefore, only using crystallographic structures to match a NP to a system is not always a reliable method, as other considerations, such as reactions and solubility, can further complicate and affect the nucleation particle activity.

## Conflicts of interest

There are no conflicts to declare.

## Data availability

The data supporting this article have been included as part of the supplementary information (SI). The SI contains supporting characterization data to support the claims of the work. This includes an image of as-received strontium chloride hexahydrate, TGA data of as-received calcium chloride hexahydrate, uncertainty analysis of undercooling based on DSC techniques, additional refined powder diffraction data from strontium chloride hexahydrate that was immersed in calcium chloride hexahydrate, and a complete DSC data set for Fig. 9. See DOI: <https://doi.org/10.1039/d5ma00906e>.

## Acknowledgements

This material is based upon work supported by the U.S. Department of Energy's Office of Energy Efficiency and Renewable Energy (EERE) under the Buildings and Technologies Award Number DE-EE0009155 and DE-EE010905.

## References

- G. A. Lane, *Solar Heat Storage: Latent Heat Materials Volume II: Technology*, CRC Press, 1986.
- M. Telkes, Nucleation of Supersaturated Inorganic Salt Solutions, *Ind. Eng. Chem.*, 1952, **44**(6), 1308–1310, DOI: [10.1021/ie50510a036](https://doi.org/10.1021/ie50510a036).
- B. Vonnegut and H. Chessin, Ice Nucleation by Sprecipitated Silver Iodide and Silver Bromide, *Science*, 1971, **174**, 945–946.
- S. Marks, An Investigation Of The Thermal Energy Storage Capacity Of Glauber's Salt With Respect To Thermal Cycling, *Sol. Energy*, 1980, **25**, 255–258.
- J. P. Elder, Thermal energy storage materials – a DSC study, *Thermochim. Acta*, 1980, **36**(1), 67–77, DOI: [10.1016/0040-6031\(80\)80110-9](https://doi.org/10.1016/0040-6031(80)80110-9).
- D. E. Oliver, A. J. Bissell, X. Liu, C. C. Tang and C. R. Pulham, Crystallisation studies of sodium acetate trihydrate – suppression of incongruent melting and sub-cooling to produce a reliable, high-performance phase-change material, *CrystEngComm*, 2021, **23**(3), 700–706, DOI: [10.1039/d0ce01454k](https://doi.org/10.1039/d0ce01454k).
- G. A. Lane, Phase change materials for energy storage nucleation to prevent supercooling, *Sol. Energy Mater. Sol. Cells*, 1992, **27**, 135–160, DOI: [10.1016/0927-0248\(92\)90116-7](https://doi.org/10.1016/0927-0248(92)90116-7).
- H. Feilchenfeld and S. Sarig, Calcium chloride hexahydrate: a phase-changing material for energy storage, *Ind. Eng. Chem. Prod. Res. Dev.*, 1985, **24**(1), 130–133, DOI: [10.1021/i300017a024](https://doi.org/10.1021/i300017a024).
- R. Pilar, L. Svoboda, P. Honcova and L. Oravova, Study of magnesium chloride hexahydrate as heat storage material, *Thermochim. Acta*, 2012, **546**, 81–86, DOI: [10.1016/j.tca.2012.07.021](https://doi.org/10.1016/j.tca.2012.07.021).
- P. J. Shamberger and T. Reid, Thermophysical Properties of Lithium Nitrate Trihydrate from (253 to 353) K, *J. Chem. Eng. Data*, 2012, **57**(5), 1404–1411, DOI: [10.1021/je3000469](https://doi.org/10.1021/je3000469).
- S. Ahmed, D. Ibbotson, C. Somodi and P. J. Shamberger, Zinc Nitrate Hexahydrate Pseudobinary Eutectics for Near-Room Temperature Thermal Energy Storage, *ACS Appl. Eng. Mater.*, 2023, **2**(3), 530–541, DOI: [10.1021/acsaenm.3c00444](https://doi.org/10.1021/acsaenm.3c00444).
- C. A. Angell and J. C. Tucker, Heat Capacities and Fusion Entropies of the Tetrahydrates of Calcium Nitrate, Cadmium Nitrate, and Magnesium Acetate. Concordance of Calorimetric and Relaxational “Ideal” Glass Transition Temperatures, *J. Phys. Chem.*, 1974, **78**(3), 278–281.
- D. Turnbull and B. Vonnegut, Nucleation Catalysis, *Ind. Eng. Chem.*, 1952, **44**(6), 1292–1298, DOI: [10.1021/ie50510a031](https://doi.org/10.1021/ie50510a031).
- V. J. Schaefer, The formation of ice crystals in the laboratory and the atmosphere, *Chem. Rev.*, 1949, **44**(2), 291–320, DOI: [10.1021/cr60138a004](https://doi.org/10.1021/cr60138a004).
- R. O. Piltz and Z. Barnea, X-ray Diffraction Study of Anharmonic Thermal Vibrations in  $\beta$ -AgI, *J. Appl. Crystallogr.*, 1987, **20**, 3–7, DOI: [10.1107/S0021889887087235](https://doi.org/10.1107/S0021889887087235).
- K. Rottger, A. Endriss, J. Ihringer, S. Doyle and W. F. Kuhs, Lattice constants and thermal expansion of H<sub>2</sub>O and D<sub>2</sub>O ice Ih between 10 and 265 K. Addendum, *Acta Crystallogr B*, 2012, **68**(1), 91, DOI: [10.1107/S0108768111046908](https://doi.org/10.1107/S0108768111046908).
- G. Roudsari, B. Reischl, O. H. Pakarinen and H. Vehkamäki, Atomistic Simulation of Ice Nucleation on Silver Iodide (0001) Surfaces with Defects, *J. Phys. Chem. C*, 2019, **124**(1), 436–445, DOI: [10.1021/acs.jpcc.9b08502](https://doi.org/10.1021/acs.jpcc.9b08502).
- H. A. Levy and G. C. Lisensky, Crystal structures of sodium sulfate decahydrate (Glauber's salt) and sodium tetraborate decahydrate (borax). Redetermination by neutron diffraction, *Acta Crystallogr. B: Struct. Sci.*, 1978, **34**, 3502–3510.
- N. Kumar and D. Banerjee, Thermal Cycling of Calcium Chloride Hexahydrate With Strontium Chloride as a Phase Change Material for Latent Heat Thermal Energy Storage Applications in a Nondifferential Scanning Calorimeter Set-Up, *J. Thermal Sci. Eng. Appl.*, 2019, **11**(5), 051014, DOI: [10.1115/1.4042859](https://doi.org/10.1115/1.4042859).



- 20 H. Schmit, D. Rudaleviciene, C. Rathgeber and S. Hiebler, Calorimetric Investigation Of Two Factors Influencing The Maximum Storage Capacity Of Calcium Chloride Hexahydrate, *presented at the IOP Conference Series: Materials Science and Engineering*, 2019.
- 21 S. Kaneff and A. Brandsetter, *Calcium Chloride Hexahydrate Formulations For Low Temperature Heat Storage Applications*, 1992.
- 22 K. Gawron and J. Schröder, Properties of some salt hydrates for latent heat storage, *Int. J. Energy Res.*, 1977, **1**(4), 351–363, DOI: [10.1002/er.4440010407](https://doi.org/10.1002/er.4440010407).
- 23 B. Carlsson, H. Stymne and G. Wettermark, An Incongruent Heat-of-Fusion System - CaCl<sub>2</sub>·6H<sub>2</sub>O - Made Congruent through Modification of the Chemical Composition of the System, *Sol. Energy*, 1979, **23**, 343–350.
- 24 J. C. O. 'C. Young and J. A. Collicutt, Low Temperature Energy Storage in Calcium Chloride Hexahydrate, *Energy Developments: New Forms, Renewables, Conservation*, 1984.
- 25 H. Kimura and J. Kai, Mixtures of Calcium Chloride Hexahydrate with Some Salt Hydrates or Anhydrous Salts as Latent Heat Storage Materials, *Energy Convers. Manage.*, 1988, **28**(3), 197–200.
- 26 A. Hassan, *Phase Change Materials for Thermal Regulation of Building Integrated Photovoltaics*, Technological University Dublin, 2010.
- 27 X. Zhang, *et al.*, Enhanced thermal conductivity in a hydrated salt PCM system with reduced graphene oxide aqueous dispersion, *RSC Adv.*, 2018, **8**(2), 1022–1029, DOI: [10.1039/c7ra10632g](https://doi.org/10.1039/c7ra10632g).
- 28 J. Charles, *Performance and Stability of CaCl<sub>2</sub>·6H<sub>2</sub>O - Based Phase Change Materials*, Doctor of Philosophy, Mechanical Engineering, Lehigh University, 2019.
- 29 J. Charles, X. Wang, C. E. Romero and S. Neti, Experimental Characterization of Low-Temperature Inorganic Phase Change Materials by Differential Scanning Calorimetry, *J. Adv. Thermal Sci. Res.*, 2019, **6**, 71–84.
- 30 H. Schmit, D. Rudaleviciene, C. Rathgeber and S. Hiebler, Influence of basic raw materials on the maximum storage capacity of the phase change material calcium chloride hexahydrate, *J. Energy Storage*, 2020, **27**, 101064, DOI: [10.1016/j.est.2019.101064](https://doi.org/10.1016/j.est.2019.101064).
- 31 M. R. Conde, Properties of aqueous solutions of lithium and calcium chlorides: formulations for use in air conditioning equipment design, *Int. J. Therm. Sci.*, 2004, **43**(4), 367–382, DOI: [10.1016/j.ijthermalsci.2003.09.003](https://doi.org/10.1016/j.ijthermalsci.2003.09.003).
- 32 D. Ibbotson, S. Ahmed and P. J. Shamberger, Mutability of Nucleation Particles in Reactive Salt Hydrate Phase Change Materials, *J. Phys. Chem. C*, 2024, **128**(41), 17282–17290, DOI: [10.1021/acs.jpcc.4c03913](https://doi.org/10.1021/acs.jpcc.4c03913).
- 33 G. Bajnóczy, Reversibility Problems of Calcium Chloride Hexahydrate - Strontium Chloride Hexahydrate Heat Stores, *Appl. Energy*, 1984, **16**, 77–82.
- 34 G. O. Assarsson and A. Balder, Equilibria between 18 and 114 in the aqueous ternary system containing Ca<sup>2+</sup>, Sr<sup>2+</sup>, and Cl<sup>-</sup>, *J. Phys. Chem.*, 1953, **57**(7), 717–722, DOI: [10.1021/j150508a028](https://doi.org/10.1021/j150508a028).
- 35 P. A. Agron and W. R. Busing, Calcium and strontium dichloride hexahydrates by neutron diffraction, *Acta Crystallogr., Sect. C: Cryst. Struct. Commun.*, 1986, **42**(2), 141–143, DOI: [10.1107/s0108270186097007](https://doi.org/10.1107/s0108270186097007).
- 36 A. T. Jensen, *On the Structure of SrCl<sub>2</sub>·6(H<sub>2</sub>O) (Matematisk-Fysiske Meddelelser - Kongelige Danske Videnskabernes Selskab)*, 1942, pp. 1–22.
- 37 W. Xu, *et al.*, SrCl<sub>2</sub>(2)·6H<sub>2</sub>O: An Alkaline-Earth-Metal Chloride Hexahydrate as Deep-Ultraviolet Nonlinear-Optical Crystal with the [Sr(H<sub>2</sub>O)(6)](2+)(infinity) Cationic Framework, *Inorg. Chem.*, 2023, **62**(27), 10523–10527, DOI: [10.1021/acs.inorgchem.3c01742](https://doi.org/10.1021/acs.inorgchem.3c01742).
- 38 J. Paris and R. Jolly, Observations sur le Comportement a la Fusion-Solidification du Chlorure de Calcium Hexahydrate, *Thermochim. Acta*, 1989, **152**, 271–278.
- 39 G. Li, B. Zhang, X. Li, Y. Zhou, Q. Sun and Q. Yun, The preparation, characterization and modification of a new phase change material: CaCl<sub>2</sub>·6H<sub>2</sub>O–MgCl<sub>2</sub>·6H<sub>2</sub>O eutectic hydrate salt, *Sol. Energy Mater. Sol. Cells*, 2014, **126**, 51–55, DOI: [10.1016/j.solmat.2014.03.031](https://doi.org/10.1016/j.solmat.2014.03.031).
- 40 D. Gao, Y. Guo, X. Yu, S. Wang and T. Deng, Thermal characteristics of room temperature inorganic phase change system containing calcium chloride, *Chem. Res. Chin. Univ.*, 2015, **31**(3), 452–456, DOI: [10.1007/s40242-015-4387-9](https://doi.org/10.1007/s40242-015-4387-9).
- 41 K. Shahbaz, I. M. AlNashef, R. J. T. Lin, M. A. Hashim, F. S. Mjalli and M. M. Farid, A novel calcium chloride hexahydrate-based deep eutectic solvent as a phase change materials, *Sol. Energy Mater. Sol. Cells*, 2016, **155**, 147–154, DOI: [10.1016/j.solmat.2016.06.004](https://doi.org/10.1016/j.solmat.2016.06.004).
- 42 X. Xu, H. Cui, S. A. Memon, H. Yang and W. Tang, Development of novel composite PCM for thermal energy storage using CaCl<sub>2</sub>·6H<sub>2</sub>O with graphene oxide and SrCl<sub>2</sub>·6H<sub>2</sub>O, *Energy Build.*, 2017, **156**, 163–172, DOI: [10.1016/j.enbuild.2017.09.081](https://doi.org/10.1016/j.enbuild.2017.09.081).
- 43 T. Zou, *et al.*, Preparation and performance of modified calcium chloride hexahydrate composite phase change material for air-conditioning cold storage, *Int. J. Refrig.*, 2018, **95**, 175–181, DOI: [10.1016/j.ijrefrig.2018.08.001](https://doi.org/10.1016/j.ijrefrig.2018.08.001).
- 44 T. Wang, X. Zhou, Z. Liu, J. Wang, Y. Zhang and W.-P. Pan, Preparation of energy storage materials working at 20–25 °C as a cold source for long-term stable operation, *Appl. Therm. Eng.*, 2021, **183**, 116220, DOI: [10.1016/j.applthermaleng.2020.116220](https://doi.org/10.1016/j.applthermaleng.2020.116220).
- 45 J. Thakkar, N. Bowen, A. C. Chang, P. Horwath, M. J. Sobkowicz and J. Košny, Optimization of Preparation Method, Nucleating Agent, and Stabilizers for Synthesizing Calcium Chloride Hexahydrate (CaCl<sub>2</sub>·6H<sub>2</sub>O) Phase Change Material, *Buildings*, 2022, **12**(10), 1762, DOI: [10.3390/buildings12101762](https://doi.org/10.3390/buildings12101762).
- 46 M. Li, *et al.*, Emerging phase change cold storage gel originated from calcium chloride hexahydrate, *Energy*, 2023, **284**, 129278, DOI: [10.1016/j.energy.2023.129278](https://doi.org/10.1016/j.energy.2023.129278).
- 47 D. O. Akamo, *et al.*, Enhanced thermal reliability and performance of calcium chloride hexahydrate phase change material using cellulose nanofibril and graphene nanoplatelet,



- J. Energy Storage*, 2024, 75, 109560, DOI: [10.1016/j.est.2023.109560](https://doi.org/10.1016/j.est.2023.109560).
- 48 X. Li, *et al.*, Phase change behavior of latent heat storage media based on calcium chloride hexahydrate composites containing strontium chloride hexahydrate and oxidation expandable graphite, *Appl. Therm. Eng.*, 2016, **102**, 38–44, DOI: [10.1016/j.applthermaleng.2016.03.098](https://doi.org/10.1016/j.applthermaleng.2016.03.098).
- 49 B. H. Toby and R. B. Von Dreele, GSAS-II: The genesis of a modern open-source all purpose crystallography software package, *J. Appl. Crystallogr.*, 2013, **46**(2), 544–549, DOI: [10.1107/s0021889813003531](https://doi.org/10.1107/s0021889813003531).
- 50 K. H. Breuer and W. Eysel, The Calorimetric Calibration of Differential Scanning Calorimetry Cells, *Thermochim. Acta*, 1982, **57**, 317–329.
- 51 T. J. Fortin, T. K. Herman, A. A. Koepke and J. D. Splett, *Certification of Standard Reference Material 2232a - Indium for DSC Temperature and Enthalpy Calibration*, Special Publication (NIST SP), 2024, DOI: [10.6028/nist.sp.260-242](https://doi.org/10.6028/nist.sp.260-242).
- 52 D. G. Archer and S. Rudtsch, Enthalpy of Fusion of Indium: A Certified Reference Material for Differential Scanning Calorimetry, *J. Chem. Eng. Data*, 2003, **48**, 1157–1163.

